Proceedings of the 7th European VLBI Network Symposium
Bachiller, R. Colomer, F., Desmurs, J.F., de Vicente, P. (eds.)
October 12th-15th 2004, Toledo, Spain

A detailed study of the nuclear region of Mrk 273

M. Bondi[1], D. Dallacasa[2], M.A. Pérez Torres[3], and T.W.B. Muxlow[4]

[1] Istituto di Radioastronomia, Via Gobetti 101, I-40129, Bologna, Italy
[2] Dipartimento di Astronomia, Università di Bologna, Via Ranzani 3, I-40127, Bologna, Italy
[3] Instituto de Astrofisica de Andalucia, CSIC, Apartado Correos 3004, 18080 Granada, Spain
[4] Jodrell Bank Observatory, University of Manchester, Macclesfield, Cheshire, SK119DL, U.K.

Abstract. We present 5 GHz EVN+MERLIN observations of the nuclear region of the ultra luminous infrared galaxy Mrk 273. These observations confirms the detection, on the mas scale, of two resolved component labelled as N and SE in the literature. We use published VLBA observations at 1.4 GHz, at the same resolution, to derive spectral index information of component N and SE and discuss these findings in relation with different hypothesis (compact starburst or AGN) for the origin of the radio emission.

1. Introduction

Ultraluminous infrared galaxies (ULIRGs) are the most luminous galaxies in the local universe with $L \geq 10^{12}$ $L_{\odot}$, comparable with quasars (Sanders et al. 1988). The bulk of the luminosity of ULIRGs is thought to be produced by dust, in the inner kpc of the galaxy, heated by a powerful source of optical-UV continuum. An important question to be answered is which is the dominant gas-heating mechanism in the ULIRGs: an active galactic nucleus (AGN) or a massive starburst? Recent developments using near-IR spectroscopy suggest enhanced star formation in the majority of the ULIRGs (Genzel et al. 1998) with a significant heating from the AGN only in the most luminous objects (Veilleux, Sanders & Kim 1999). Radio observations can prove to be extremely important in studying the central region of ULIRGs since they are unaffected by dust extinction and allow for sub-parsec resolution using VLBI techniques. The most spectacular evidence of a compact starbust in a ULIRG is indeed the discovery of a population of bright radio supernovae in the nuclear region of Arp 220 (Smith et al. 1998) detected at 1.6 GHz.

Mkn 273 is a ULIRG at $z = 0.0378$ classified as a Seyfert 2 and/or LINER. It is a merging galaxy showing a disturbed morphology on the kpc scale. The nuclear region of Mkn 273 is extremely complex and has been studied in details in the radio (Cole et al. 1999, Carilli & Taylor 2000, Yates et al. 2000), NIR (Knapen et al. 1997), optical (Mazzarella & Boroson 1993), and X–ray band (Xia et al. 2002). Three extended radio components (N, SE and SW, see Fig. 1 in Yates et al. 2000) are detected within 1 arcsecond in the nucleus of Mkn 273. These are all physically related components, probably associated with the merging process, and not the result of chance projection of background sources.

The three components show different morphologies and properties. Component SW is the weaker one and is barely detected only with MERLIN at 18 cm. Component N and SW have bright NIR counterparts (Knapen et al. 1997; Majewski et al. 1993) and are redder than component SE, suggesting the presence of strong star formation in these 2 components, while component SE is not detected in the NIR.

Throughout this contribution we will assume $H_0 = 75$ km s^{-1} Mpc^{-1}. At the distance of Mrk 273, 1 mas corresponds to 0.7 pc. To put this in perspective with other ULIRGs or starburst galaxies where the origin of the radio emission has been investigated, Mrk 273 is at about twice the distance of Arp 220 and 56 times the distance of M 82.

2. The radio view of the nuclear region in Mrk 273

In this section we will focus on published results from high resolution radio imaging of components N and SE in Mrk 273. MERLIN observations at 5 GHz have resolved component N into two compact regions (we will refer to them as N1 and N2 for the western and eastern components, respectively) embedded in diffuse emission while component SE is barely resolved.

VLBA+VLA observations at 1.4 GHZ have provided the best images of Mrk 273 obtained so far (Carilli & Taylor 2000). At a resolution of 50 mas (see fig. 1) two things can be immediately noted from the comparison of the 1.4 and 5 GHz images: 1) the different spectral properties of component N1 and N2, N1 is stronger than N2 at 1.4 GHz but the opposite is true at 5 GHz; 2) the 300 mas ($\sim$ 210 pc) long tail of extended emission detected at 1.4 GHz in the SE component is missing from the 5 GHz image.

At a resolution of 10 mas (see fig. 2a), component N1 is still compact while N2 is resolved in multiple sub-mJy compact components which form a structure roughly elongated in north south direction. The faint halo of extended emission is punctuated by others weak and compact components. N1 is the brigtest component ($\simeq$ 3 mJy/beam) and is possibly identified with a weak AGN (but see below). Carilli & Taylor (2000) identify the compact components in N2 with brightness between 0.5 and 0.9 mJy/beam ($T_b \geq 3 \times 10^6$ K, $L_{1.4\mathrm{GHz}} \geq 10^{21}$ W Hz^{-1}) with nested supernovae remnants (SNR) and/or luminous radio supernovae (SN). To account for the observed luminosity of these compact features, assuming they are nested SNR, 10 or more of the most luminous M82-type SNR would

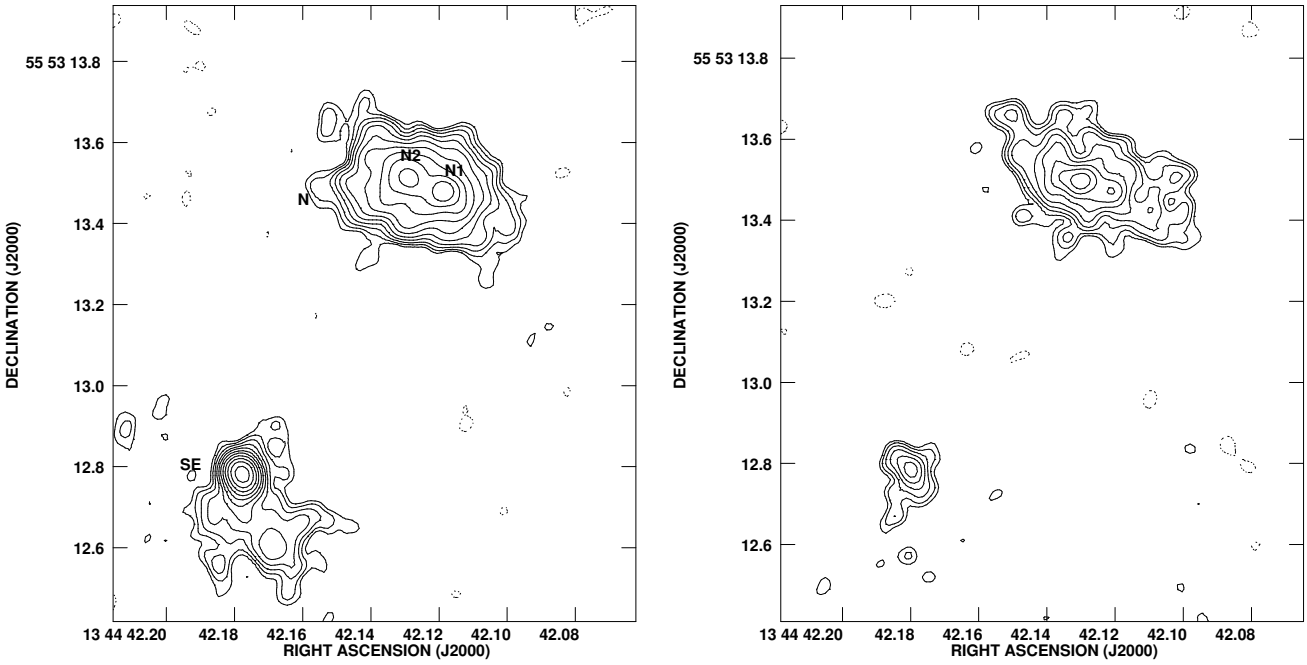

Fig. 1. *a) Left:* Image of Mrk 273 at 1.37 GHz obtained by the VLBA+VLA at 50 mas resolution. The contour levels are a geometric progression in the square root of 2, starting from 0.25 mJy/beam. The peak surface brightness is 10 mJy/beam and the off-source noise rms is 85 μJy/beam. The labels indicate the two sub-arcsecond scale compact component N and SE, and the two peaks of emission N1 and N2 inside N. *b) Right:* Image of Mrk 273 at 5 GHz obtained by MERLIN at 50 mas resolution. The contour levels are a geometric progression in the square root of 2, starting from 0.20 mJy/beam. The peak surface brightness is 4.2 mJy/beam and the off-source noise rms is 63 μJy/beam.

be required in regions less than 10 mas (7 pc) in size, while assuming that the compact sources are SN they would be extremely luminous, an order of magnitude higher than those observed in M 82 and comparable to the supernovae candidates observed in Arp 220.

The interpretation of the radio morphology of component SE is less straightforward (see fig. 3a): it shows an elongated structure in N-S about 40 mas long embedded in a weak halo, consistent with an amorphous jet or a very compact starburst. The lack of NIR emission in component SE could argue in favour of the AGN interpretation for this source, but the possibility that component is still obscured at 2.2 μm can not be ruled out.

3. EVN+MERLIN Observations

In order to investigate the complex nature of Mrk 273 we obtained EVN+MERLIN observations at 5 GHz. EVN observations were carried out at 512 Mbit/s sustained bit rate to exploit the large bandwidth capabilities of the EVN, with an array which included all the european antennas. These were the first observations at 5 GHz for the resurfaced Lovell telescope. Mrk 273 was observed in phase-reference mode for a total on-source time of 5.5 hours. The compact source J1337+550 was observed every 5 minutes as phase reference, while OQ208 and J1310+322 were used to calibrate the bandpass. Data reduction was performed using the Astronomical Image Processing System (AIPS). Standard a priori gain calibration was performed using the measured gains and system temperatures of each antenna. The amplitude calibration was refined using the phase reference source. EVN and MERLIN data sets were reduced separately and then combined to produce final images with a resolution of 10×10 arcsec and 50×50 arcsec to be compared with the 1.4 GHz images from Carilli & Taylor which we have obtained by the authors. The low resolution image is shown in Fig. 1b, while high resolution images of component N and SE are given in Fig. 2b & 3b.

4. Results and Discussion

In this section we present preliminary results from the EVN+MERLIN observations at 5 GHz. Using the 1.4 GHz images published in Carilli & Taylor (2000), and kindly provided by the authors, we have derived the spectral index between 1.4 and 5 GHz and discuss the origin and spectral properties of the emission detected in components N and SE in Mrk 273. We use the notation $S \propto \nu^{-\alpha}$.

4.1. Component N in Mrk 273

The northern source in Mrk 273 consists of two region of compact emission, coincident with the N1 and N2 components of the lower resolution MERLIN image, embedded in diffuse emission of roughly the same extension of that detected at

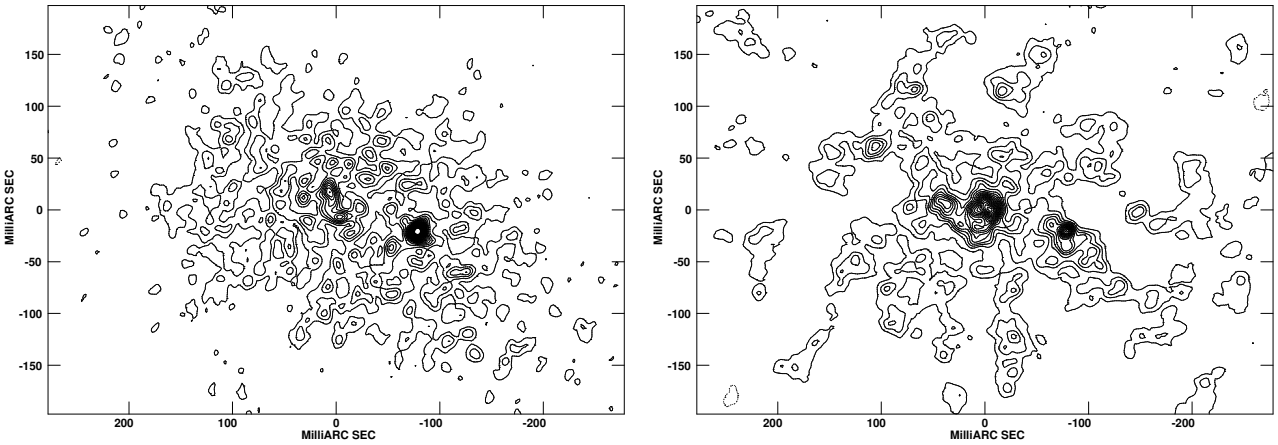

Fig. 2. *a) Left:* VLBA+VLA image of component N at 1.37 GHz at 10 mas resolution. The contours are $-1, 1, 2, 3, 4, \ldots \times 0.1$ mJy/beam. The peak surface brightness is 3.05 mJy/beam and the off-source noise is 36 μJy/beam. *b) Right:* EVN+MERLIN image of component N at 5 GHz at 10 mas resolution. The contours are $-1, 1, 2, 3, 4, \ldots \times 0.04$ mJy/beam. The peak surface brightness is 0.74 mJy/beam and the off-source noise is 15 μJy/beam.

1.4 GHz by Carilli & Taylor. It has been supposed, in the literature, that N1 hosts a weak AGN nucleus and N2 is a very compact region of massive star formation. This view is supported by two major points: 1) the detection of high excitation IR lines (Genzel et al. 1998) and hard X-ray emission (Xia et al. 2002) are evidences of an AGN-like nucleus in Mrk 273; 2) the CO emission and NIR peaks are spatially coincident with N2 (Downes & Solomom 1998, Knapen et al. 1997).

At 5 GHz, N1 is very weak (0.6 mJy/beam compared with the 3 mJy/beam at 1.4 GHz) yielding to a very steep spectral index $\alpha \simeq 1.2$. Fitting the component with elliptical gaussian and using the total flux density instead of the peak brightness doesn't change significantly the spectral index. This is clearly surprising, and would rule out the presence of an AGN nucleus in N1, unless we consider variability as a possible explanation. It is interesting to note that at the full resolution of the EVN array ($\simeq$ 5 mas), N1 is slightly resolved and elongated suggesting a core jet morphology. Deeper observations with an increased uv-coverage are necessary to resolve the N1 component.

On the other hand, the eastern component, N2, has a very complex morphology with a flat spectral index $\alpha \simeq 0.15$. The flat spectral index can be explained as the result of several compact, partly overlapping, components with spectra peaking at a few GHz and free-free absorption. The radio morphology of this region is indeed indicative of multiple compact components in a region of about 25 pc, and this is also consistent with the results from CO and NIR emission observations which indicate this region as the core of an extremely rich star forming region. Downes & Salomon (1998) derive an IR luminosity of about $6\times10^{11} L_{\odot}$ generated in a region with a radius of only 120 pc and a current molecular mass of $1\times10^{9}\ M_{\odot}$. This means that the entire molecular core has a radius 5 times that of W51 (a Giant Molecular Cloud in our galaxy), but with $\sim$ 3000 times the molecular mass and $\sim 10^5$ times the luminosity from OB stars.

The extended emission has a steep spectral index $\alpha \simeq 0.8$. Following Condon (1992) the FIR flux ($\log(FIR) = 11.6 L_{\odot}$) can be used to estimate the star formation rate, $\dot{m} \simeq 40\ M_{\odot}\mathrm{yr}^{-1}$, with a corresponding supernovae rate $\nu_{SN} \simeq 2\ \mathrm{yr}^{-1}$. These values have been derived using simple scaling law relationship to estimate starburst characteristics in terms of the star formation rate, the lower and upper mass limits to the initial mass function, $m_l \sim 5M_{\odot}$ and $m_u \sim 28M_{\odot}$, and the starburst timescale, $\Delta t_{SB} \sim 10^8$ yr. Such a supernovae rate would produce a non-thermal luminosity of 2×10^{23} W Hz^{-1} at 1.4 GHz. The observed value is 2.2×10^{23} W Hz^{-1}, in agreement with the predicted one, and so it supports the hypothesis that the extended emission is produced by elecrons which have diffused away from the SNR shocks.

4.2. Component SE in Mrk 273

In the past it has been suggested that this is a background source, but evidence for gas infall in the HI 21 cm absorption image and the low probability of a chance projection are against the background source hypothesis (Carilli & Taylor 2000). The 1.4 GHz images do not clarify if the source is core jet (and hence AGN driven) or a compact starburst, and observations in other bands don't provide a unique interpretation. At 5 GHz, the SE component is resolved in an arc-shaped radio emission resembling a core twin-jet source. The most striking peculiarity of the SE component is the steep spectral index. The integrated value is $\alpha \simeq 1.4$ with values ranging from 0.9 to 1.6 across the source. At the full resolution of the EVN observations (5 mas) the source is completely resolved out confirming the absence of any high brightness radio feature as already noted by Carilli & Taylor (2000).

5. Summary

We have reduced and analyzed 5 GHz EVN+MERLIN observations of the ULIRG Mrk 273. Both the sub-arcsecond scale compact nuclei, N and SE, were detected and resolved. Using published images at 1.4 GHz we have derived the spectral index of the radio emitting regions reaching the following results:

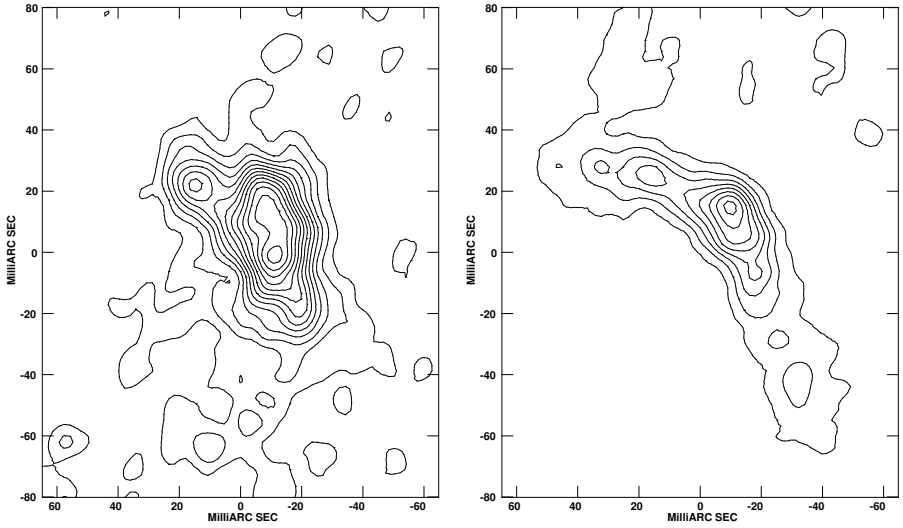

Fig. 3. *a) Left:* VLBA+VLA image of component SE at 1.37 GHz at 10 mas resolution. The contours are $-1, 1, 2, 3, 4, \ldots \times 0.1$ mJy/beam. The peak surface brightness is 1.35 mJy/beam and the off-source noise is 36 μJy/beam. *b) Right:* EVN+MERLIN image of component SE at 5 GHz at 10 mas resolution. The contours are $-1, 1, 2, 3, 4, \ldots \times 0.04$ mJy/beam. The peak surface brightness is 0.34 mJy/beam and the off-source noise is 15 μJy/beam.

1. The compact component N1, often indicated as a possible AGN nucleus, has a very steep spectral index ($\alpha \simeq 1.2$). Unless strong flux density variability has occurred between the two epochs of observation this result is difficult to reconcile with the AGN hypothesis.
2. The component N2 is partly resolved in several compact radio sources. The integrated spectral index of this region is flat ($\alpha = 0.15$) probably because of the superposition of several components with peaked spectra and/or free-free absorption. This is consistent with findings in the NIR which identify N2 as a compact region with the strongest star formation.
3. The spectral index of the extended emission in component N is typical of non-thermal optically thin radio emission ($\alpha \simeq 0.8$), and the luminosity of the extended emission is consistent with being produced by electrons diffused away from supernova remnants in a luminous starburst.
4. The SE component has a very steep spectrum ($\alpha \simeq 1.4$), with no compact high brightness component.

Acknowledgements. We thank Chris Carilli for the processed VLBA images at 1.4 GHz of Mrk 273, and the staff at JIVE for the efforts spent during the correlation and pipeline of these data.

References

Carilli, C.L., & Taylor, G.B. 2000, ApJ, 532, L95
Cole, G.H.J., Pedlar, A., Holloway, A.J., Mundell, C.G., 1999, MNRAS, 310, 1033
Condon, J.J., 1992, ARAA, 30, 575
Downes, D., Solomon, P.M., 1998, ApJ, 507, 615
Genzel, R., Lutz, D., Sturm, E., et al. 1998, ApJ, 498, 579
Knapen, J.H., Laine, S., Yates, J.A., et al. 1997, ApJ, 490, L29
Majewski, S.R., Hereld, M., Koo, D.C., Illingworth, G.D., Heckman, T.M., 1993, ApJ, 402, 125
Mazzarella, J.M., & Boroson, T.A. 1993, ApJS, 85, 27
Sanders, D.B., Soifer, B.T., Elias, J.H., et al. 1988, ApJ, 325, 74
Smith, H.E., Lonsdale, C.J., Lonsdale, C.J., Diamond, P.J., 1998, ApJ, 493, L17
Veilleux, S., Sanders, D.B., Kim, D.C., 1999, ApJ, 522, 113
Xia, X.Y., Xue, S.J., Mao, S., et al. 2002, ApJ, 564, 196
Yates, J.A., Richards, A.M.S., Wright, M.M., et al. 2000, MNRAS, 317, 28